

An Equilibrium Point based Model Unifying Movement Control in Humanoids

Abstract—Despite all the dynamics methods effectively used in robotics control, few tackle the intricacies of the human musculoskeletal system itself. During movements, a huge amount of energy can be stored passively in the biomechanics of the muscle system. Controlling such a system in a way that takes advantage of the stored energy has led to the Equilibrium-point hypothesis (EPH). In this paper, we propose a two-phase model based on the EPH. Our model is simple and general enough to be extended to various motions of all body parts. In the first phase, gradient descent is used to obtain one kinematics endpoint in joint space, given a task in Cartesian space. In the second phase where the movements are actually executed, we use damped springs to simulate muscles to drive the limb joints. The model is demonstrated by a humanoid doing walking, reaching, and grasping.

I. INTRODUCTION

Humans and other primates can easily perform a wide variety of tasks without much knowledge about themselves and the environment. This contrasts with the current state of robotics: even for a robot to reach to a position with natural pose can be a research topic, much less for the robot to be as dexterous and intelligent as humans. In our research, we use a virtual humanoid from Boston Dynamics Inc. Although the virtual guy can perform a repository of motions, it is not an adaptive and intelligent agent. The reason lies in the fact that the virtual guy is simply playing back the motion data captured from humans. When it encounters new environments or tasks, it does not have the ability to plan new movements. Even within the method of playing back captured motion data, mismatch and unrealistic movements are highly possible due to various reasons as sensor errors, calibration errors, and other metric difference between the virtual model and real humans.

One of the central questions of studying human movements is how the Central Nervous System (CNS) calculates the motor commands to drive the limb. One proposal, derived from robotics, is that the brain computes inverse dynamics solutions. In movement control, the task is usually described in Cartesian space, which is different from the actual space where the motor commands are executed. Therefore, a proper coordinate transformation is required to find the solution in the joint space given a task in Cartesian space, which is well known as inverse dynamics. This problem turns out to be quite difficult, because the musculoskeletal system typically has many more degrees of freedom (DOFs) than the task constraints at hand. Among the inverse dynamics methods, one approach is to study movement control as a formal optimization problem as exemplified in [18] [13] [22]. Some researchers tried to solve the same problem by adding constraints to the redundancy as

in [21] [24] [19]. Most of those approaches can only be applied to simple robots with known geometry and in static environments. Few models are eligible to be used in robot systems as complicated as humans in dynamic environments. The inverse dynamics calculation for an anthropomorphic robot with more than 30 DOFs requires extremely high computation.

Contrary to the inverse dynamics force control model, Equilibrium Point Hypothesis is another theoretical framework used by a lot of researchers in human motor control. Feldman [6] [7] pioneered the EPH that limb movements could be achieved by shifting the limb posture represented as equilibrium from one position to another. Researchers put forward the theory and proposed many more 'dialects' of EPH [3] [4] [10]. The central idea of EPH spring model discriminates movement planning from execution. Motor planning is to program the movement tasks by choosing a succession of discrete equilibrium points (EPs). Once these points are chosen, in the execution phase the muscle spring system moves without further direction under CNS control.

Whether it is EPH or inverse dynamics that really controls human movements is a subject of controversy. Many researchers argue against the EPH by providing experimental evidence [12] [16]. Feldman and other researchers defended the EPH in various reference [5] [8] [9]. With all those debates, most of EPH researchers' attention has been attracted to prove the validity of the theory. Little research has been directed to study how humans choose those EPs for a given task. Less work is devoted to demonstrate how the simple EPH mechanism can be applied to control human motions. In this paper, we propose a two-phase control model based on the idea of the EPH. Given a task in Cartesian space, we first develop a motor simulation model to plan the EPs in joint space. We specifically address the following two questions: first, how are EPs calculated to achieve a particular motor goal? Second, how are EPs planned in motor synergy to satisfy multiple goals in complex movements? During the movement execution, damped springs are used to simulate muscles to actually drive the movements. We demonstrate that the model is a general model that can unify the control of various motions, such as reaching, walking and hand movements.

In the next section, we describe the details of the model in the context of a simple reaching task. Section II demonstrate the humanoid doing a diverse of complex motions. We finally conclude the paper and discuss avenues for future work.

II. MODEL DESCRIPTION

Our model suggests that human movements can be planned in segments, and each segment has an equilibrium end-point in joint configuration. Before the movements are initiated, the end-point is calculated using the motor planning model elaborated below, and then used to set muscle lengths, modeled as damped springs' natural lengths, for movement execution. During movement planning, the lest amount of necessary equilibrium points is calculated for a motor task. For example, in simple voluntary arm movements, only final EP is probably required. But in more complicated movements as obstacle avoidance, more than one EPs are necessary. Movements are generated by shifting from one segment EP to the next.

A. Motor planning

Given a task in Cartesian space, the first step of our model is to get a kinematics solution in joint space. To do so, a recent suggestion has been to steer to the end point using gradient descent of an objective function that expresses variation of the distance between the current handtip position to the destination [23]. Although we were able to replicate their results, in our experience this method is delicate and very sensitive to its various parameter settings. Besides, their pure gradient descent method can have unrealistic trajectories as shown in Fig. 2. However, it serves as the starting point for our method which uses the gradient method, not to actually control the movement execution, but instead in simulation to generate end configurations in joint space that are then used by subsequent processing stages.

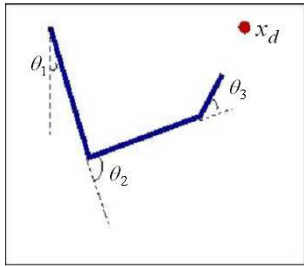


Fig. 1. Reaching task in a 2D space with a 3 DOF system.

Consider a three joint limb moving in a vertical plane as shown in Fig. 1. Let X , the task space, be the set of points that can be reached by the arm in the plane. Let Θ , the configuration space or joint space, be a subset of R^3 , and it specifies all the possible postures. There exists a vector function f , which maps Θ onto X , i.e., every hand location $x \in X$ can be written as $f(\theta)$ for at least one $\theta \in \Theta$, and every θ maps to a certain $x \in X$. The objective function is defined as the distance from current end effector position $f(\theta)$ to the destination x^D as in Equ. (1).

$$r(\theta, x^D) = \sqrt{\sum_{i=1}^2 (x_i^D - f_i(\theta))^2} \quad (1)$$

Bringing the hand to the destination consists of repeatedly computing gradient of the objective function and changing the posture a small amount for each step until the hand reaches the destination. The gradient function in Equ. (2) is a vector, and each component specifies how much to change each joint value to bring the hand closer to the target. β is a scaling factor to adjust the amount of changes of each time step. $J(f(\theta))$ is the Jacobian matrix.

$$d\theta = -\beta \frac{(x - f(\theta)) \times J(f(\theta))}{\sqrt{\sum_{i=1}^2 (x_i^D - f_i(\theta))^2}} \quad (2)$$

We regenerate the results of [23] in Fig. 2. Blue configurations are the postures obtained by doing gradient descent to the objective function for each step, and the green curve gives the trajectory generated. There are at least two factors that make their method nonbiological. First, the trajectory goes through a big curve and follows a line going back to the destination, which is not what we observe in human reaching movements. Second, the end posture shown in bold blue lines does not fit with the human posture in the same task.

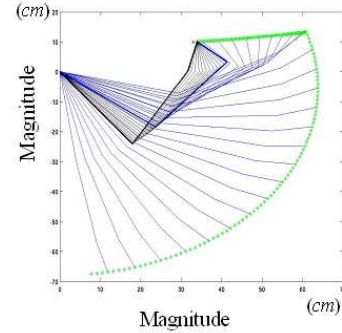


Fig. 2. End posture planning. A) Blue curves: gradients of the distance function for each time step. B) Black curves: energy optimization steps to get the realistic end point.

To solve the final posture problem, we take the idea of energy minimization. The same idea has been studied by [1] [17]. Different from the energy in their methods, we minimize the potential energy during the planning phase, instead of the kinetic energy which will not be available until the movements begin. We assume that the potential energy is at least proportional to the energy required for the movements, even if it does not represent the exact energy consumption during the execution. We define another cost function given in Equ. (3) using Lagrange multiplier method for the constraint optimization problem. The goal is to minimize the first part, which is the potential energy, while keeping the second part, which constraints the end effector to the destination, to be zero. The black configurations in Fig. 2 illustrate how the joint configurations gradually changing from the blue bold one to the final biological end posture shown in black bold lines.

$$E(\theta) = Mgh(\theta) + \lambda(f(\theta) - x^D) \quad (3)$$

where, M is the total mass of the limb. $h(\theta)$ is the height of the limb's center of gravity (COG), and it is a function of the current limb configuration θ . g is the gravity parameter. The term of $Mgh(\theta)$ is the potential energy of the limb system. $f(\theta)$ is the current end effector position, and x^D is the destination. λ is the parameter for the constraint function in Lagrange multiplier method [2].

B. Spring model

Human movements are driven by the flexion and extension of muscles. Among the models to describe muscle properties, one widely-used model is proposed by Hill in [14] [15]. A muscle produces two kinds of forces, elastic and viscous. The sum of those two forces composes the muscle's total force. The passive element of a muscle has an elastic property and can be simply modeled as a spring. The elastic force varies directly with the distance that is elongated from its resting length. The formula is given in Equ. (4):

$$F_e = K \times (l - l_r) \quad (4)$$

where, F_e is the elastic force, l_r and l are the spring's resting length and actual length, respectively. K is called the spring constant or stiffness.

The molecular structure of a muscle causes it to display a property of viscosity, that is, the resistance to move. This resistive force is like a shock absorber [20]. If you push the piston sitting over a fluid in an encapsulated bucket, the shock absorber will resist by a tension of F_v that depends on the viscosity B of the fluid. The faster you push the piston, the stronger resistant force the fluid generates. The relation between the speed of pushing and the force can be written in Equ. (5)

$$F_v = B \times \dot{l} \quad (5)$$

where, \dot{l} is the velocity of the spring length. Combining the two properties, the force produced by an active muscle is a function of both the muscle length and its rate of changing as represented in Equ. (6).

$$F = K \times (l - l_r) + B \times \dot{l} \quad (6)$$

where K and B are the spring stiffness and viscosity parameters respectively.

C. Movement execution

The dynamics system of the limb system in Fig. 1 can be usually expressed in Equ. (7).

$$\tau = I(\theta)\ddot{\theta} + C(\theta, \dot{\theta})\dot{\theta} + G(\theta) \quad (7)$$

where τ is a 3×1 vector of torques applied to shoulder, elbow and wrist, $I(\theta)$ is a 3×3 matrix representing the kinetic energy, $C(\theta, \dot{\theta})$ is a 3×3 matrix of centrifugal and Coriolis effects, $G(\theta)$ is a 3×1 vector of gravitation. θ , $\dot{\theta}$, and $\ddot{\theta}$ are vectors of joint values, velocities and accelerations.

In inverse dynamics methods, for each time step, certain torques are computed to drive the limb to move along a planned trajectory represented as a series of joint values, velocities and accelerations. This involves a considerable amount of

computation even in a simple 3 DOF system. In our model, to actually drive the arm movements, we set the springs as in Fig. 3, where each spring controls one degree of freedom and produces the amount forces as in Equ. (6). The joint space solution obtained during the planning phase allows the ready determination of the spring natural lengths. As far as the spring length l is not equal to the natural length l_r , forces are generated to attract the joint configurations to the end point. Comparing to the inverse dynamics methods, springs take charge of the movement control once the natural lengths are set and generate proper torques to drive the limb to the destination.

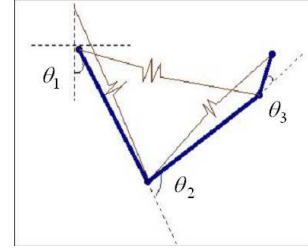


Fig. 3. Three damped springs controlling a 3 DOF system

Fig. 4 shows four snapshots of the arm moving from the initial position to the destination. In the simulation, we use constant spring stiffness and viscosity parameters during the process of reaching. Different sets of parameters will generate different reaching movements, and we manually adjust the parameters to simulate the realistic reaching. To further study how close our simulation is to human reaching, we captured some human movement data in the same task and compare them to the simulation results. Fig. 6 presents the reaching trajectory and speed profiles comparison. Solid lines are the captured human data, and the dashed lines are the model prediction. We get fairly good fitting of the two, and the model generates the tuning curves in speed profiles typically observed in human reaching movements.

Reaching with avoidance is always a subject of research. In our model, reaching with avoidance can be easily implemented by adding one more EP during planning, which is the position where to avoid the obstacle. We assume the robot system knows the obstacle position, and the 3D via point is chosen beyond certain distance from the obstacle. Motor planning algorithm is used to calculate the EP in joint space with respect to the via point. Then movements are achieved by setting the two EPs consecutively. How the robot observes the obstacle's position would involve vision systems, and is beyond the subject of this paper. Fig. 5 gives the snapshots of reaching while avoiding the desk.

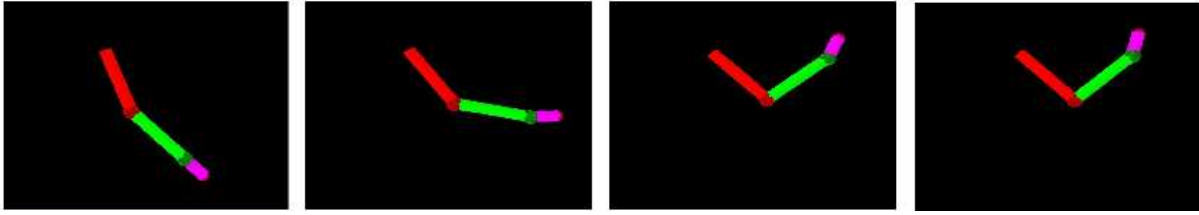


Fig. 4. Reaching movement executed.

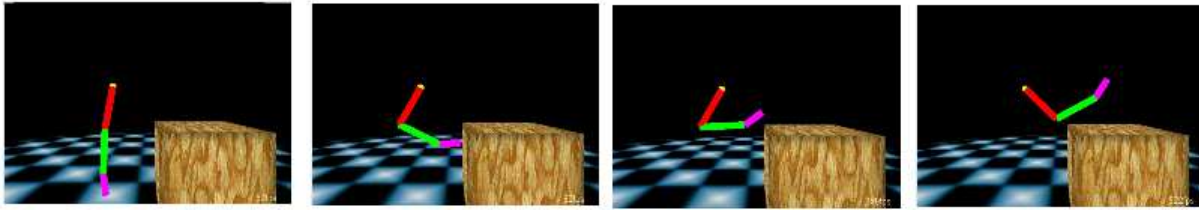


Fig. 5. Reaching movement while avoiding the desk.

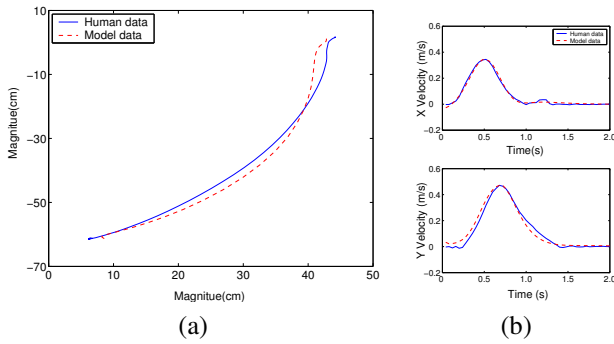


Fig. 6. Model simulation and human movement comparison. (a) end effector trajectory. (b) speed profiles.

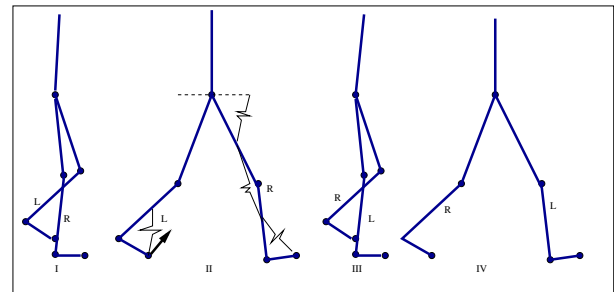


Fig. 8. Four EPs for one cycle of walking

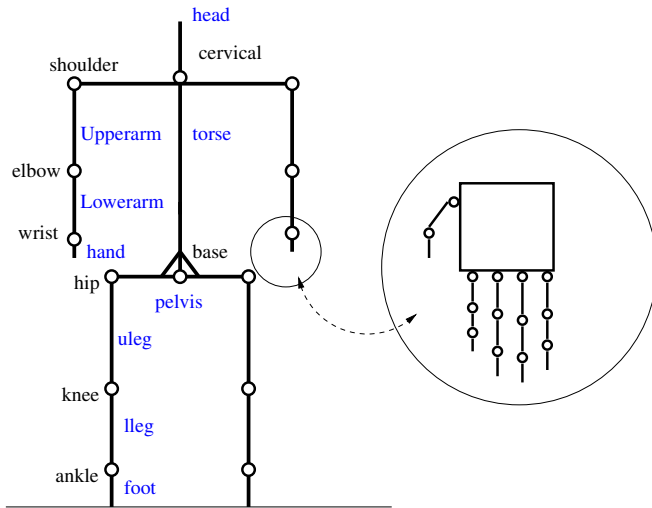


Fig. 7. Humanoid skeleton structure.

III. HUMANOID SIMULATION

We build a 33 DOF humanoid as in Fig. 7. Each leg has three joints: hip, knee and ankle, and each joint has one DOF. Each arm has six DOFs, three DOFs for the shoulder, one for the elbow and the other two for the wrist. Torso has one DOF for leaning forward or backward. Currently, the head is not involved in the movement control. The humanoid has one hand with 14 DOFs.

A. Walking

We divide one cycle of walking into four segments, and each segment has one endpoint configuration. Natural and realistic walking is generated by shifting from one endpoint to the next. For regular walking, humans control the movements within the body coordinate, thus the motor planning mapping the 3D task space to human joint space is not necessary. The walking introduced in this paper belongs to this category. Walking with obstacle avoidance would require the planning phase to calculate the leg joint configurations with respect to the obstacle in 3D space. Till this point, we did not implement the function yet. The four EPs are defined after analyzing

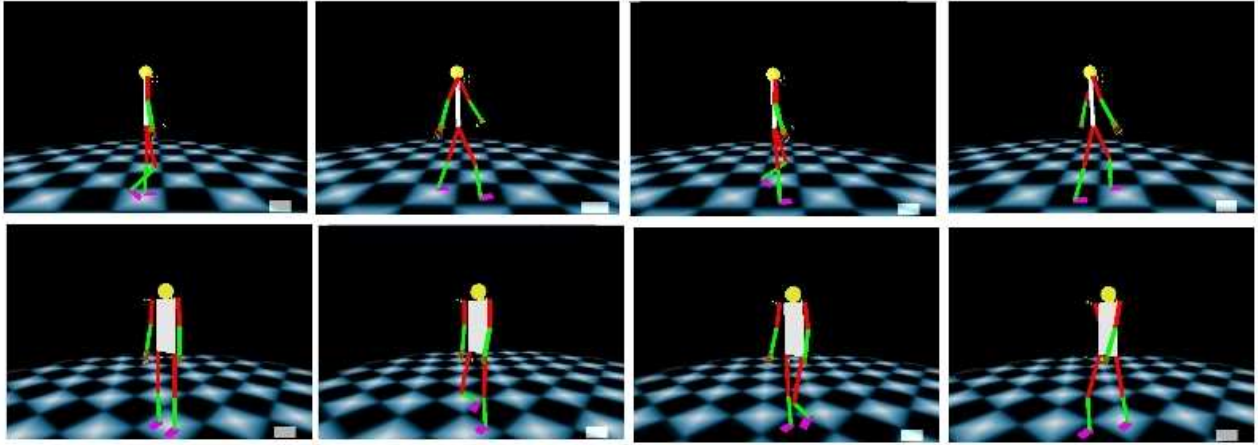


Fig. 9. Humanoid walking with coordinated whole body movements

the human walking data from Boston Dynamics Inc. Fig. 8 specifies the four EPs for one cycle of walking, and each leg has three damped springs to control the contraction and extension of the hip, knee and ankle.

During walking simulation, one technical difficulty is to keep the humanoid's balance along the walking direction. When the springs pull the robot's legs forward, the torso is always legged behind, since the body has no outsider force to provide the forward speed. The robot always ends up falling backwards. We solve this problem by instantly pushing the back foot on the ground. The counterforce from the ground will provide the body a forward speed. In the implementation, the pushing force is produced by setting the back ankle's spring natural length to a larger value for a short period, when the front foot gets contact with the ground. This way, the body's COG shifts from the back foot to the front. This is also the mechanism humans use during walking. Fig. 9 shows the snapshots of the humanoid walking with whole body coordinated.

B. Hand movements

In this part, we demonstrate the model to control the hand grasping and manipulation of objects. We build a 14 DOF hand as in Fig. 7, where thumb has 2 DOFs and the rest of fingers each has 3 DOFs. Grasping based on the EP model is much easier than traditional robotics methods, where precise finger positions on the object needs to be planned ahead of time. Fuentes [11] used different predefined grasping plans for different types of regular objects, and a genetic algorithm to plan the finger tip positions on an irregular object. In our case, planning can be done by setting the finger EPs into the object. On one hand, this strategy can greatly simplify the planning computation compared to Fuentes' planning algorithms. On the other hand, it provides the necessary force and friction to

manipulate the object when the finger tips get contact with the object. How much contact force to exert on the object can be adjusted by the stiffness of the finger springs.

Fig. 10 shows the hand grasping a cylinder, and releasing it. This is a simple demonstration of the model applied to the hand doing grasping and manipulation. The hand is a simplified version of human hand. The goal of this part is to illustrate that our EP based model is a general and simple enough model to be applied to hand control. To synthesize more complex hand and objects interactions, we need to build the hand closer to human hand by adding a heading rotation to each finger, and two more rotations to the thumb. Grasping and manipulation of sphere, cubic or other kinds of objects can be implemented easily based on this EP model.

IV. CONCLUSION AND FUTURE WORK

A. Conclusion

We discuss the limitations of traditional inverse dynamics methods applying to an anthropomorphic robot to generate complex behaviors in a physical world. Based on equilibrium-point hypothesis, we develop a two-phase control model that is general enough to control a diversity of motions involving any parts of human body. Our major contribution is in presenting a novel human movement control model that can unify various both simple and complex human motions. Besides, our model are inspired from findings of human movement research, and can serve as a candidate to further study human movements. Till this point, most of human control models are restricted to simple movements in 2D space within very small scope. To further study human motions, models that can accommodate large movements in 3D space is indispensable. Our model can

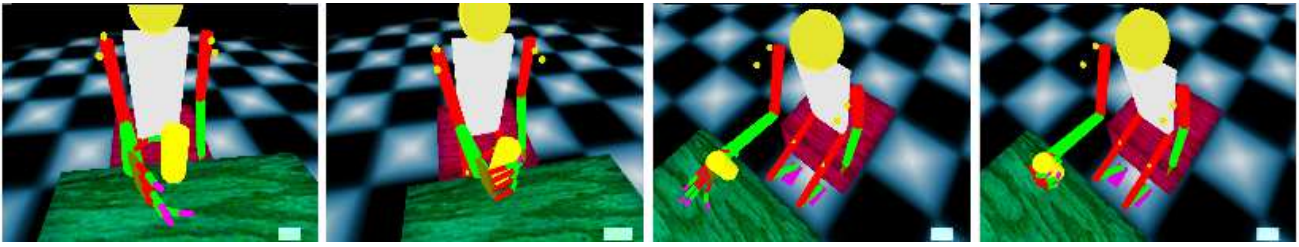


Fig. 10. Humanoid reaching and grasping the object.

be viewed as a test-bed to human movement research, as well as a humanoid robot to demonstrate its capability.

From the aspect of both robotics and human movement modeling, one of the biggest advantage of the EP based model is their low computation requirement. For example, electro-mechanical systems that use direct servoing, such as ATR's SARCOS system, require rates as high as 10KHz to implement inverse control methods, while cortical neurons' signaling is typically in the range of 10 to 100 Hz. Thus any biologically plausible method of control should respect the low sampling rates available. The only computation of the EP model is to choose a succession of discrete EPs. Once these points are chosen, the muscle spring system moves without further guidance under the control.

B. Future work

Till this point, we only build a prototype of the control model, and scratch the surface of the research that can be done based on the model. With the graphics humanoid, we want to build motor movement units, such as protective stepping and arm reaction when falling down, different rising after a fall, balancing etc. Learning algorithms can be attempted to learn the mapping between the state space to the action control. The humanoid will be studied how to autonomously react to dynamic environments. Another direction can be motor learning. Instead of the traditional motor learning of trajectories or dynamics, we can have robot learn the EPs from observing the teacher's behaviors. For example, for a mimic robot to repeat the demonstrator's reaching movement, the only parameters it has to learn are the end posture and spring parameters. This greatly reduces the amount of information and computation conveyed to the learner, and simplifies the process.

REFERENCES

- [1] R. McN. Alexander. A minimum energy cost hypothesis for human arm trajectories. *Biological Cybernetics*, 76:97–105, 1997.
- [2] Dimitri P. Bertsekas. *Constrained Optimization and Lagrange Multiplier Methods*. Academic Press, 1982.
- [3] E. Bizzi, N. Accornero, W. Chapple, and H. Hogan. Arm trajectory formation. *Exp. Brain Res.*, 46:139–143, 1982.
- [4] E. Bizzi, F. A. Mussa-Ivaldi, and S. Giszter. Computations underlying the execution of movement: a biological perspective. *Science*, 253:287–291, 1991.
- [5] A. Feldman and M. Latash. Testing hypotheses and the advancement of science: recent attempts to falsify the equilibrium point hypothesis. *Exp. Brain Res.*, 161:91–103, 2005.
- [6] A. G. Feldman. Functional tuning of the nervous system with control of movement or maintenance of a steady posture. ii. controllable parameters of the muscle. *Biophysics*, 11:565–578, 1966.
- [7] A. G. Feldman. Functional tuning of the nervous system with control of movement or maintenance of a steady posture. iii. mechanographic analysis of execution by man of the simplest motor tasks. *Biophysics*, 11:766–775, 1966.
- [8] A. G. Feldman. Once more on equilibrium-point hypothesis (λ model) for motor control. *J. Motor Behavior*, 18:17–54, 1986.
- [9] A. G. Feldman, D. J. Ostry, M. F. Levin, P. L. Gribble, and A. B. Mitnitski. Recent tests of the equilibrium-point hypothesis (λ model). *Motor Control*, 2:189–205, 1998.
- [10] T. Flash. The control of hand equilibrium trajectories in multi-joint arm movements. *Biological Cybernetics*, 57:257–274, 1987.
- [11] Olac Fuentes. *Behavior-Based Dexterous Manipulation: The Virtual Tool Approach*. PhD thesis, University of Rochester, 1997.
- [12] H. Gomi and M. Kawato. Equilibrium-point control hypothesis examined by measured arm-stiffness during multi-joint movement. *Science*, 272:117–120, 1996.
- [13] C. M. Harris and D. M. Wolpert. Signal-dependent noise determines motor planning. *Nature*, 394:780–784, 1998.
- [14] A.V. Hill. The heat of shortening and the dynamic constants of muscle. *Proceedings of Royal Society B*, 126:136–195, 1938.
- [15] A.V. Hill. The series elastic component of muscle. *Proceedings of Royal Society B*, 137:399–420, 1950.
- [16] M. R. Hinder and T. E. Milner. The case for an internal dynamics model versus equilibrium point control in human movement. *Journal of Physiology*, 549(3):953–963, 2003.
- [17] T. Kashima and Y. Isurugi. Trajectory formation based on physiological characteristics of skeletal muscles. *Biological Cybernetics*, 78:413–422, 1998.
- [18] M. Kawato. Internal models for motor control and trajectory planning. *Current Opinion in Neurobiology*, 9:718–727, 1999.
- [19] C. Phillips and N. Badler. Interactive behaviors for bipedal articulated figures. *ACM Computer Graphics*, 25(4):359–362, 1991.
- [20] R. Shadmehr and M.A. Arbib. A mathematical analysis of the force-stiffness characteristics of muscles and the role of reflexes in control of a single joint system. *Biological Cybernetics*, 66:463–477, 1992.
- [21] N. Sundar. Dexterous robotic hands: Kinematics and control. Master's thesis, Indian Institute of Technology, 1983.
- [22] E. Todorov and M. Jordan. Optimal feedback control as a theory of motor coordination. *Nature Neuroscience*, 5(11):1226–1235, 2002.
- [23] E. Torres and D. Zipser. Reaching to grasp with a multi-jointed arm. i. computational model. *Journal of Neurophysiology*, 88:2355–2367, 2002.
- [24] J. Zhao and N. Badler. Inverse kinematics positioning using nonlinear programming for highly articulated figures. *ACM Transactions on Graphics*, 13(4):313–336, 1994.